UNDERSTANDING THE STRATOSPHERIC POLAR VORTEX: A PARAMETER SENSITIVITY ANALYSIS ON A SIMPLE MODEL OF STRATOSPHERIC DYNAMICS

A Thesis

Presented to

The Faculty of the Department of Mathematics and Statistics

Sam Houston State University

In Partial Fulfillment

of the Requirements for the Degree of

Master of Science

---

by

Kiara Sanchez

May, 2020

UNDERSTANDING THE STRATOSPHERIC POLAR VORTEX: A PARAMETER SENSITIVITY ANALYSIS ON A SIMPLE MODEL OF STRATOSPHERIC DYNAMICS

by

Kiara Sanchez

APPROVED:

Edward Swim, PhD
Committee Director

John Alford, PhD
Committee Member

Luis David Garcia Puente, PhD
Committee Member

John Pascarella, PhD
Dean, College of Science and Engineering Technology

DEDICATION

I dedicate this thesis to my two parents, who both immigrated to the United States from the Dominican Republic; to my siblings and my nieces, who all mean the world to me; and to all of my best friends, who have waited for me patiently to finish.

ABSTRACT

Sanchez, Kiara, *A Parameter Sensitivity Analysis on a Simple Model of Stratospheric Dynamics*. Master of Science Thesis, Department of Mathematics and Statistics, May 2020, Sam Houston State University, Huntsville, Texas.

With the aim of understanding what drives the behavior of the stratospheric polar vortex in the Northern Hemisphere, we conduct a parameter sensitivity analysis on a simple model of stratospheric dynamics. This research will allow us to understand when and which parameters exert significant influence on the overall dynamics. Thus giving way to what potentially might drive the changes in the stratospheric polar vortex.

KEY WORDS: Polar Vortex, Stratospheric Dynamics, Parameter Sensitivity, Rossby Waves.

ACKNOWLEDGEMENTS

I would like to thank my thesis advisor Dr. Edward Swim for all of his endless help and support throughout this process. I would also like to thank the Math and Climate Research Network Summer School and Academic Year Engagement Program for initiating my work. And many thanks to my ongoing collaborators, Dr. Chris Jones, *University of North Carolina Chapel Hill*, Dr. Christian Sampson, *University of North Carolina Chapel Hill*, Ligia Flores, *Sam Houston State University*, Yorkinoy Shermatova, *University of Minnesota*, Penny Wu, *Arizona State University*, and Julie Sherman, *University of Utah*.

TABLE OF CONTENTS

LIST OF TABLES

LIST OF FIGURES

CHAPTER 1

Introduction and Motivation

1.1 A Brief Background on the Atmosphere

The atmosphere is vertically divided into four horizontal layers. The first being the troposphere which extends from the earths surface up to about 15km altitude. Most of earths weather occurs in the troposphere [1]. The stratosphere extends from the top of the troposphere (known as the tropopause) up to about 50 km altitude. The stratopause serves as the upper bound of the stratosphere and above the stratopause is the mesosphere which extends up until about 85-90km. The mesopause bounds the mesosphere and above it is the thermosphere which extends to about 600km high [1].

The forces that act on the parcels of air in the atmosphere are the pressure gradient force, the force of gravity, and the force of friction (or viscosity). The Coriolis force changes the direction of the motion of wind in the atmosphere, but has no influence on speed. In the northern hemisphere specifically, the Coriolis force acts to the right of the wind direction [8]. "The approximate balance between the pressure gradient force and the Coriolis force gives us geostrophic [wind] [8]," which provides us with a reasonable starting point for modeling the actual atmospheric wind, at least outside the tropics. But this idealization must be refined in order to understand the evolving dynamics of polar vortices, since in a broad sense, atmospheric circulation is driven by temperature and pressure gradients [5]. These effects, along with gravity and viscosity, are the starting point for most partial differential equation models for atmospheric phenomena. Here we focus on the Arctic polar vortex within the stratosphere.

1.2 The Stratospheric Polar Vortex in the Northern Hemisphere

Many of the drastic changes in weather that have been observed in recent years have been attributed to climate change. It is common that when winter days are warmer than usual, and summer days are hotter than usual, people attribute such unusual warmth to *global warming*. Though, when extreme cold is experienced, people tend to question *where is global warming, if it is getting colder than usual?* In their paper "What is the Polar Vortex and How Does It Influence Weather?" Darryn W. Waugh, Adam H. Sobel, and Lorenzo M. Polvani claim that more recently, especially after the winter of 2014, climatologists and weathermen have attributed this extreme cold to the *polar vortex* [9]. They go on to explain how attributing such cold to the *polar vortex* is misguided and misleading, based on differences in hemispheres and layers of the atmosphere.

In particular, Waugh, Sobel, and Polvani begin by clarifying the existence of a polar vortex in the northern hemisphere and the existence of another distinct polar vortex in the southern hemisphere. Thus, referring to the *polar vortex* as a singular phenomena is both misguided and misleading. In both the northern hemisphere and in the southern hemisphere, there exists a polar vortex in the troposphere and another one in the stratosphere [9]. Reports on the weather typically focus on events within the troposphere, but the vortices within this layer are not completely independent of changes in the stratosphere.

All of the polar vortices are natural parts of the earth's climate system. They have always existed. Waugh, Sobel and Polvani claim that a more informed answer is that some of these extreme weather events may be linked to a shift in the location of the tropospheric polar vortex and/or the stratospheric polar vortex since, "the larger topographic and land-sea contrasts in the northern hemisphere generate stronger upward propagating waves than in the southern hemisphere, causing the northern stratospheric vortex to be weaker and more distorted than its southern counterpart [9].” Hence, this paper will focus on studying the stratospheric polar vortex in the northern hemisphere.

As noted before, atmospheric circulation is driven by both pressure and temperature gradients. Hence, the temperature gradient in the winter is normally strong, as the poles are typically much colder than the tropics, which keeps the jet stream and subsequently the tropospheric polar vortex where one would normally expect. However, as we have seen in more recent years, the poles are warming at a much faster rate than the rest of the earth due to climate change. Hence, the temperature gradient is not as strong. This weakening of the temperature gradient is suspected to be weakening the polar front, or jet stream, which typically keeps the tropospheric polar vortex above the tropical latitudes. However, since this temperature gradient has lessened, the jet stream has weakened, and it is suspected that this has allowed the tropospheric polar vortex to travel further south than we would normally expect - leading to the extreme cold weather events that we have experienced in the northern parts of the United States.

There is no clear connection between how the stratospheric polar vortex directly influences the weather that we experience here on earth [9]. Thus fully understanding stratospheric dynamics is the key first step for any hopes of understanding how it exerts influence on weather and possibly how it causes changes in the tropospheric polar vortex.

It is important to note that Rossby waves, also known as planetary waves, are the fundamental disturbances in the stratosphere. In his work "A Simple Model of Stratospheric Dynamics Including Solar Variability," Alexander Ruzmaikin provides a simple dynamic model consisting of three ordinary differential equations to study the interaction of planetary (or Rossby) waves with zonal winds in the stratosphere [7]. In the next chapter we will analyze Ruzmaikin's model and its development.

CHAPTER 2

Modeling a Stratospheric Polar Vortex

2.1 Stratospheric Vacillation Cycles

In 1976, James R. Holton and Clifford Mass published *Stratospheric Vacillation Cycles*. In this work, they note that, "it is generally agreed that most planetary waves in the stratosphere are produced and maintained by vertical propagation of wave energy from the troposphere," and many dynamical and mechanistic models have confirmed such phenomena. Though, on the other hand, there are wave-mean flow oscillations in the stratosphere which occur on a 1-4 week cycle throughout the winter which at the time were observed through data and some stratospheric simulation models, but for which an origin had not yet been fully understood. Hence, they developed and studied a simple mechanistic model to show that, "wave-mean flow oscillations in the stratosphere may exist even when the tropospheric forcing is completely steady." Holton and Mass used a quasi-geostrophic β-plane channel model with a sine jet meridional variation for their mean zonal wind. They assumed that the mean zonal flow was confined to a β-plane channel centered at 60°N with meridional extent of 60° latitude. They then go on to define specific upper, lower, and side boundaries for their model. After analyzing the solution regimes for their model, Holton and Mass conclude that their model conveys that large-scale stratospheric motions can indeed experience vacillations even when the tropospheric forcing is steady [4].

2.2 Bifurcation Properties

In the 1987 paper, *Bifurcation Properties of a Stratospheric Vacillation Model*, Shigeo Yoden explores the model mentioned in the previous section. Yoden assumes that the Newtonian heating is zero at the upper boundary and that the amplitude of the wave forcing at the bottom boundary is constant (to replicate steady forcing). Further, he decomposes the equation for the conservation of quasi-geostrophic potential vorticity into two differential equations for computational convenience. Applying the method of finite differences, he reduces the model to a set of 81 nonlinear ordinary differential equations. With this system in hand, Yoden completes a full bifurcation analysis of the system, including, but not limited to finding the critical points of the system and analyzing their stability and type. He finds that there are three branches of steady solutions, two of which coexist at certain values of the wave forcing which represent the system being close to radiative equilibrium and the system undergoing vacillations, respectively. The periodic solutions Yoden finds come from the steady solutions undergoing a Hopf bifurcation [10].

2.3 Seasonal and Interannual Variations of the Stratospheric Circulation

In 1990, Yoden published further work that he did on the model developed by Holton and Mass. This time, in *An Illustrative Model of Seasonal and Interannual Variations of the Stratospheric Circulation*, Yoden varied the radiative heating periodically to try to mimic and understand seasonal and interannual variability of the stratosphere. Yoden notes that, "seasonal variation is the atmospheric response to the annual forcing by solar radiation." Yoden also recognizes that there is large interannual variability in the stratosphere during winter in the high latitudes of the northern hemisphere that is closely related to whether a stratospheric sudden warming occurs in the winter. He goes on to explain that this interannual variability of the stratosphere has been attributed to a number of phenomena, including but not limited to variations of the boundary conditions like the influence of the quasi-biennial oscillation, variations of planetary waves in the troposphere, variations of the intensity of the Hadley circulation, and finally, variations of solar activity. For all of the phenomena he explains, Yoden contends that there are not enough observations to confirm what causes the interannual variability. Hence, in this paper he uses the simple wave-zonal flow interaction model that he used in his 1987 paper, but this time to illustrate the seasonal and interannual variations of the stratosphere in both hemispheres. His analysis of the model reveals that the response of the stratosphere to radiative heating depends on the magnitude of wave forcing at the bottom boundary. That is, when the wave forcing is small, "there are rapid transitions of the zonal mean quantities after the equinoxes." During the transitions, wave activity is high and has a minimum in midwinter. But, when the wave forcing is large, there is always vacillation and a series of stratospheric sudden warmings. Yoden notes that a further study with a more realistic model should be conducted in order to get a more valid explanation for the seasonal and interannual variations of the stratosphere [11].

2.4 A Simple Model of Stratospheric Dynamics Including Solar Variability

The paper, *A Simple Model of Stratospheric Dynamics Including Solar Variability*, by Ruzmaikin, *et al.*, provides a simple dynamic model for studying stratospheric dynamics including planetary waves, zonal wind, seasonal variations and solar variability [7]. The authors use the model that Holton and Mass created and Yoden developed, and further simplified it into three ordinary differential equations by considering only one vertical layer within the stratosphere. They first follow the same development of the model as in [4], [10] and [11]. In these previous papers, a specific location for the lower boundary is not defined. They claim that the specification of such a location does not quantitatively affect the model, however, it may change how one qualitatively interprets the results. Hence, this new model identifies a lower boundary condition at $z = 0$, which allowed a reduction of the system to just the three ordinary differential equations. Similar to Yoden, Ruzmaikin then applies the method of finite differences, but instead of Yoden's detailed approach, with only the simplest case where only three distinct z-values are used within the stratosphere – one at the lower boundary ($z = 0$), one at the upper boundary, and one intermediate value, denoted $z = z_T$. This results in the ability to reduce the system to three ordinary differential equations [7]:

$$\dot{X} = -X/\tau_1 - rY + sUY - \xi\Psi_0 + \delta_w\dot{\Psi}_0, \tag{1}$$

$$\dot{Y} = -Y/\tau_1 - rX + sUX + \zeta\Psi_0 U, \tag{2}$$

$$\dot{U} = -(U - U_R)/\tau_2 - \eta\Psi_0 Y - \delta_\Lambda\dot{\Lambda}. \tag{3}$$

We will be using this system as the basis of our study. In Table 1, we define the variables and parameters within the model. Unless otherwise noted, parameter values are found in [7].

Using a simple model such as this one allows us to investigate it analytically and can provide us with a basic physical intuition of stratospheric dynamics without the need for large computer resources. As Ruzmaikin mentioned, this system allows the study of the long-term dynamics/behavior by revealing the following: (1) the interaction between waves and zonal wind, (2) some of the same properties Holton and Mass observed, and (3), the

$x(t)$	Azimuthal coordinate
$y(t)$	Latitudinal coordinate
$u(t)$	Wind speed
τ_1	Dimensionless time parameter, approx. 1.060×10^7
τ_2	Dimensionless time parameter, approx. 2.624×10^6
r	Dimensionless frequency parameter, approx. 7.276×10^{-6}
s	Dimensionless parameter, inversely proportional to length, approx. 3.083×10^{-7}
ξ	Dimensionless scaling parameter, approx. 1.492×10^{-3}
ζ	Dimensionless parameter, inversely proportional to speed, approx. 2.784×10^{-3}
η	Dimensionless parameter, inversely proportional to length, approx.2.605×10^{-13}
δ_w	Dimensionless time parameter, approx. 5.223×10^3
δ_Λ	Dimensionless parameter, directly prop. to time and length, approx. 3.128×10^3
$\Psi_0(t)$	Wave stream function at the lower stratospheric boundary
k	Wavenumber corresponding to the azimuthal coordinate x
l	Wavenumber corresponding to the latitudinal coordinate y
U_R	Mean radiative zonal wind
f_0	Coriolis parameter at latitude 60°N
β	Meridional derivative of the Coriolis parameter
H	Mean scale height
$h(t)$	Wave Amplitude
g	Gravitational acceleration
$\Lambda(t)$	Gradient of the mean radiative zonal wind
N^2	Buoyancy parameter
ρ	Density
α	Newtonian cooling/heating rate

Table 1: State variable, parameters, and functions used within the model (1)-(3).

transition between atmospheric states which further reveals the occurrence of warm and cold winters [7]. The reduced system also allows for the study of long-term behavior rather than just short-term behavior, which reveals more of the overall dynamics.

Stratospheric dynamics are largely influenced by an interaction between vertically propagating waves from the troposphere and winds in the stratosphere. Hence, Ruzmaikin's model is well suited for studying the dynamics of the stratosphere because it incorporates planetary waves, zonal wind, and their interaction.

2.5 Explicitly Defining Functions Within the Model

Ruzmaikin, Lawrence, and Cadavid did not explicitly define a function for $\Lambda(t)$. Although, they noted that $\Lambda(t) = \frac{dU_R}{dz}(t)$ which allowed us to look back into the foundational papers and find an explicit functtion for Λ. In his paper *An Illustrative Model of Seasonal and Interannual Variations of the Stratospheric Circulation*, Shigeo Yoden defined $\frac{dU_R}{dz}(t) = 0.75 - 2.25\cos\omega_a t[\times 10^{-3}s^{-1}]$ where $\omega_a = \frac{2\pi}{365}$ is a frequency of annual variation, and the unit of time t is day. Similarly, Ruzmaikin, Lawrence, and Cadavid did not define Ψ_0 explicitly. However, they did state that $\Psi_0 = \frac{g}{f_0}h(t)$. Thus, we were able to find a function defined as h, and use it in this expression to have a function for Ψ_0. In that paper, Yoden defined $h_B(t) = 130 + 30\cos\omega_i t[m]$ with 0.0459 day$^{-1} \leq \omega_i \leq$ 0.0823 day^{-1} [11].

$U_R(z,t)$ is the mean zonal wind in radiative equilibrium and $h_B(t) = \Psi(0,t)\frac{f_0}{g}$ is the wave amplitude at the bottom boundary where f_0 is the Coriolis parameter and g is the gravitational acceleration [7]. Hence it is of critical importance that we preserve the behavior of these functions in our systems of differential equations since the physical role they play in driving stratospheric dynamics is important. In the next section, we illustrate that role numerically.

2.6 Transient and Steady-State Properties of the State Variables

The following three figures display the solutions, X, Y, and U, to the equations 1, 2, and 3, respectively. These solutions were generated using the ODE45 function in Matlab, all with an initial condition of zero. The plots reveal that there is a periodicity to the dynamics, which is in fact tied to the functions Ψ_0 and Λ. However, all solutions become close to a steady-state value within one year. Moreover, each solution includes a sharp gradiant near $t \approx 50$, which led to instability in the sensitivity analysis. Based on the parameter values in Table 1 and the nature of the transient solutions observed within the first 365 days, it appears that the parameters δ_w and δ_Λ, coefficients on the derivatives of Ψ_0 and Λ, respectively, have the most influence on the dynamics of the system initially.

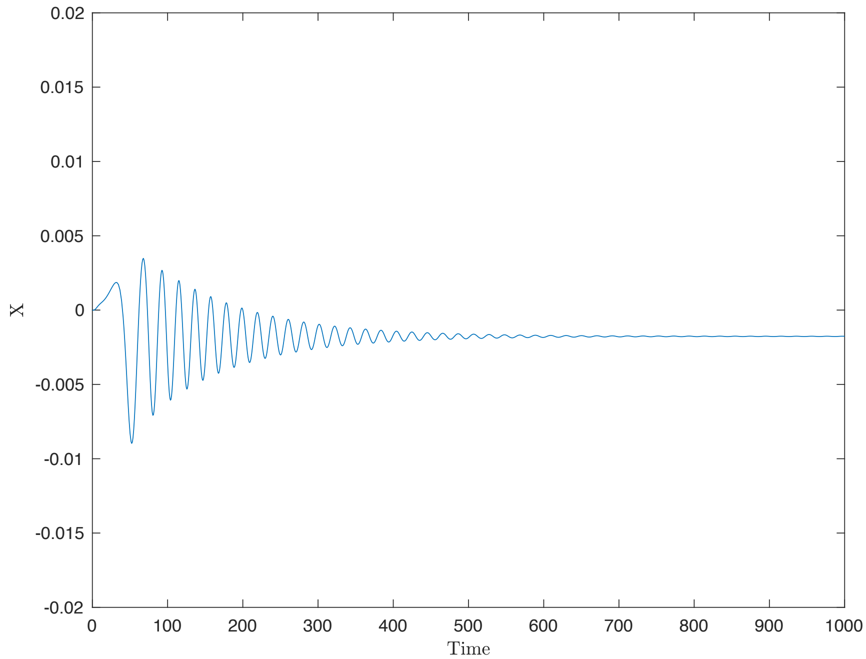

Figure 1: Plot of the azimuthal coordinate variable over time.

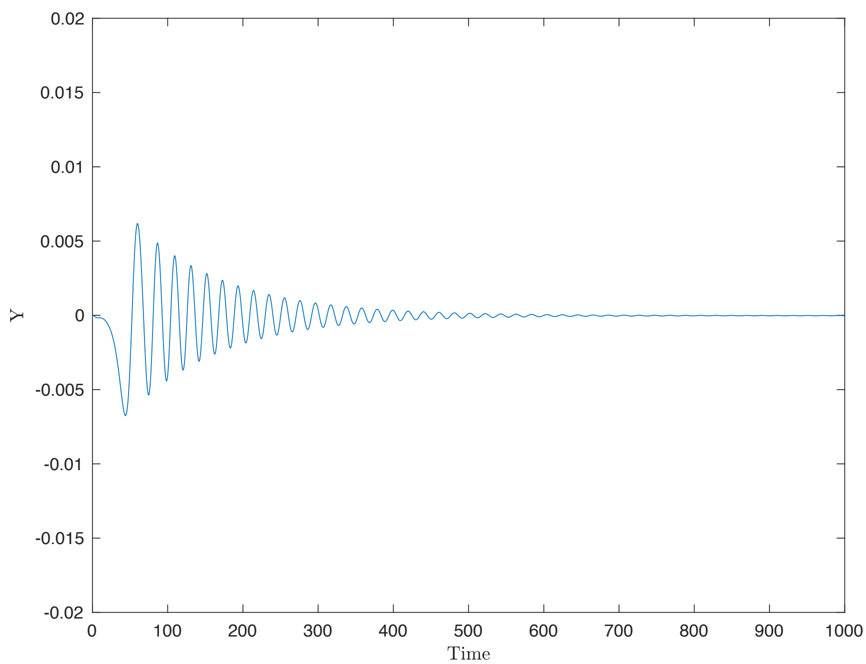

Figure 2: Plot of the latitudinal coordinate variable over time

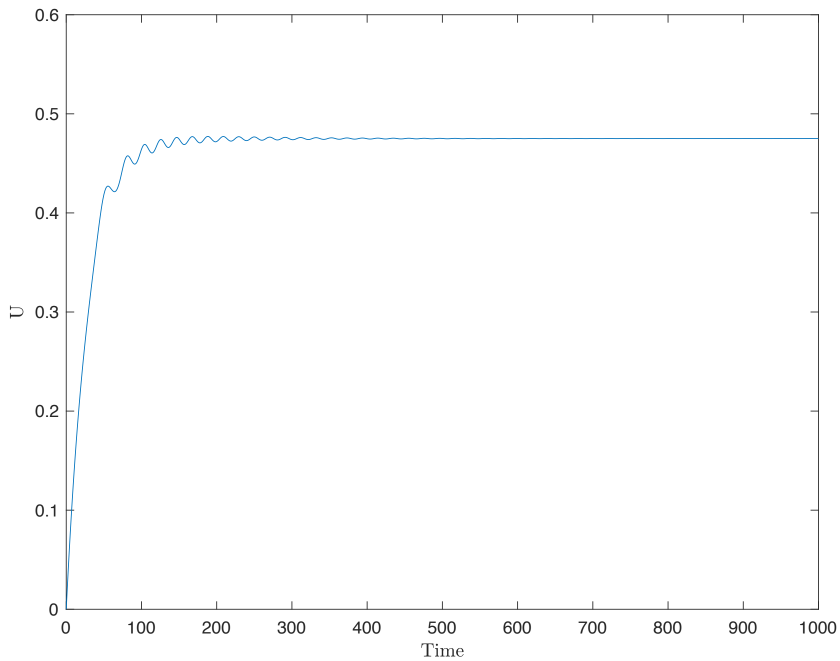

Figure 3: Plot of the wind speed variable over time

In the next section dimensional analysis is performed on the model. This allows us to confirm that the functions Ψ_0 and Λ were well suited to be used in Rozmaikin, Lawrence, and Cadavid's model.

2.7 Dimensional Analysis

Dimensional analysis allows one to understand the relationships of the quantities in the equations and their dimensional homogeneity [6]. What follows is the dimensional analysis we performed on the system of ODEs with the functions Λ, h, and Ψ_0 defined previously. We begin with the material properties listed in Table 1, which are then used to construct parameters in our system of ODEs as described in [7]. These are then used to validate each term with the differential equations.

$$[f_0] = \tfrac{1}{T}, \quad [g] = \tfrac{L}{T^2}, \quad [z_T] = L, \quad [N] = \tfrac{1}{T}, \quad [k] = \tfrac{1}{L}, \quad [l] = \tfrac{1}{L}$$
$$[\Lambda] = \tfrac{1}{T}, \quad [\beta] = \tfrac{1}{LT}, \quad [h] = L, \quad [U_B] = \tfrac{L}{T}, \quad [\alpha] = \tfrac{1}{T}, \quad [H] = L$$

The equations $a(1)-a(9)$, and $b(1)-b(4)$ below are listed in the appendix of [7]. They are used to then develop the parameters used directly in the model. Thus we first had to perform a dimensional analysis on these relationships to then determine the dimensions of the parameters in the differential equations.

$$a(1) = k^2 + l^2 + \frac{f_0^2}{N^2}(\frac{1}{4H^2} + \frac{8}{z_T^2})$$

$$[a(1)] = (\frac{1}{L})^2 + (\frac{1}{L})^2 + \frac{(\frac{1}{T}^2)}{(\frac{1}{T}^2)}(\frac{1}{L^2} + \frac{8}{L^2}) = (\frac{1}{L})^2 + (\frac{1}{L})^2 + 1(\frac{1}{L^2} + \frac{1}{L^2})$$

$$a(2) = \frac{f_0^2}{N^2}[\frac{1}{2H}\frac{\partial\alpha}{\partial z} - \alpha(\frac{1}{4H^2} + \frac{8}{z_T^2})]$$

$$[a(2)] = \frac{(\frac{1}{T}^2)}{(\frac{1}{T}^2)}[\frac{1}{L}\frac{1}{TL} - \frac{1}{T}(\frac{1}{L^2} + \frac{1}{L^2})] = 1[\frac{1}{TL^2} - \frac{1}{TL^2} + \frac{1}{TL^2}]$$

$$a(3) = -k\beta$$

$$[a(3)] = \frac{1}{L}\frac{1}{LT} = \frac{1}{L^2T}$$

$$a(4) = \frac{8k}{3\pi}\frac{f_0^2}{N^2}(\frac{2}{z_T} - \frac{1}{2H})$$

$$[a(4)] = \frac{1}{L}\frac{(\frac{1}{T}^2)}{(\frac{1}{T}^2)}(\frac{1}{L} - \frac{1}{L}) = \frac{1}{L} \times 1(\frac{1}{L} - \frac{1}{L})$$

$$a(5) = \frac{8k}{3\pi}\frac{f_0^2}{N^2}(\frac{4}{z_T^2} + \frac{1}{Hz_T})$$

$$[a(5)] = \frac{1}{L}(\frac{1}{T}^2)(\frac{1}{T}^2)(\frac{1}{L^2} + \frac{1}{LL}) = \frac{1}{L}(\frac{1}{L^2} + \frac{1}{L^2}) = \frac{1}{L^3} + \frac{1}{L^3}$$

$$a(6) = \frac{8k}{3\pi}[k^2 + \frac{f+0^2}{N^2}(\frac{1}{4H^2} + \frac{4}{z_T^2} - \frac{1}{Hz_T})]$$

$$[a(6)] = \frac{1}{L}[\frac{1}{L^2} + \frac{(\frac{1}{T}^2)}{(\frac{1}{T}^2)}(\frac{1}{L^2} + \frac{1}{L^2} - \frac{1}{LL})] = \frac{1}{L^3} + \frac{1}{L^3} + \frac{1}{L^3} - \frac{1}{L^3}$$

$$a(7) = \frac{f_0^2}{N^2}\frac{g}{z_T f_0}(-\frac{\partial\alpha}{\partial z} + \frac{4\alpha}{z_T})$$

$$[a(7)] = \frac{(\frac{1}{T}^2)}{(\frac{1}{T}^2)}\frac{\frac{L}{T^2}}{L\frac{1}{T}}(\frac{1}{TL} + \frac{\frac{1}{T}}{L}) = 1\frac{L}{T^2}\frac{T}{L}(\frac{1}{TL} + \frac{1}{T}\frac{1}{L}) = \frac{1}{T^2L} + \frac{1}{T^2L}$$

$$a(8) = \frac{4f_0^2}{z_T^2N^2}\frac{f}{f_0}$$

$$[a(8)] = \frac{\frac{1}{T^2}}{L^2\frac{1}{T^2}} \times \frac{\frac{L}{T^2}}{\frac{1}{T}} = \frac{1}{T^2}\frac{T^2}{L^2}\frac{L}{T^2}\frac{T}{1} = \frac{1}{LT}$$

$$a(9) = \frac{32k}{3\pi z_T^2}\frac{f_0^2}{N^2}\frac{g}{f_0}$$

$$[a(9)] = \frac{\frac{1}{L}}{L^2}\frac{\frac{1}{T^2}}{\frac{1}{T^2}}\frac{\frac{L}{T^2}}{\frac{1}{T}} = \frac{1}{L^3}\frac{L}{T} = \frac{1}{L^2T}$$

$$b(1) = l^2 + \frac{f_0^2}{N^2}(\frac{4}{z_T^2} + \frac{1}{Hz_T})$$

$$[b(1)] = \frac{1}{L^2} + \frac{\frac{1}{T^2}}{\frac{1}{T^2}}(\frac{1}{L^2} + \frac{1}{L^2}) = \frac{1}{L^2} + \frac{1}{L^2} + \frac{1}{L^2}$$

$$b(2) = \frac{f_0^2}{N^2}[\frac{1}{z_T}\frac{\partial\alpha}{\partial z} - \alpha(\frac{4}{z_T^2} + \frac{1}{HZ_T})]$$

$$[b(2)] = \frac{\frac{1}{T^2}}{\frac{1}{T^2}}[\frac{1}{L}\frac{1}{TL} - \frac{1}{T}(\frac{1}{L^2} + \frac{1}{L^2})] = \frac{1}{TL^2} - \frac{1}{TL^2} + \frac{1}{TL^2}$$

$$b(3) = -\frac{16kl^2}{3\pi z_T^2}\frac{f_0^2}{N^2}\frac{g}{f_0}\exp\frac{z_T}{2H}$$

$$[b(3)] = \frac{\frac{1}{L}\frac{1}{L^2}}{L^2}\frac{\frac{1}{T^2}}{\frac{1}{T^2}}\frac{\frac{L}{T^2}}{\frac{1}{T}}\frac{L}{L} = \frac{1}{L^3}\frac{1}{L^2}\frac{L}{T^2}\frac{T}{1} = \frac{1}{L^5}\frac{L}{T} = \frac{1}{TL^4}$$

$b(4) = -\frac{f_0^2}{N^2}(\frac{1}{2H} - \frac{2}{z_T})$

$[b(4)] = 1(\frac{1}{L} - \frac{1}{L})$

Now we can calculate the dimensions of the parameters in the model. The formulas of the parameters using $a(1) - a(9)$ and $b(1) - b(4)$ listed below are employed again from the appendix of [7].

$[\zeta] = [\frac{a(9)}{a(1)}] = \frac{\frac{1}{L^2T}}{\frac{1}{L^2}} = \frac{1}{L^2T}\frac{L^2}{1} = \frac{1}{T}$ $\quad [\eta] = [\frac{b(3)}{b(1)}] = \frac{\frac{1}{TL^4}}{\frac{1}{L^2}} = \frac{1}{TL^4}\frac{L^2}{1} = \frac{1}{TL^2}$

$[\tau_1] = [\frac{a(1)}{a(2)}] = \frac{\frac{1}{L^2}}{\frac{1}{L^2T}} = \frac{1}{L^2}\frac{L^2T}{1} = T$ $\quad [s] = [\frac{a(6)}{a(1)}] = \frac{\frac{1}{L^3}}{\frac{1}{L^2}} = \frac{1}{L^3}\frac{L^2}{1} = \frac{1}{L}$

$[r] = [\frac{a(3)+a(4)\Lambda+a(5)U_B}{a(1)}] = \frac{\frac{1}{L^2T}+\frac{1}{L^2}\frac{1}{T}+\frac{1}{L^3}\frac{L}{T}}{\frac{1}{L^2}} = \frac{\frac{1}{L^2T}+\frac{1}{L^2T}+\frac{1}{L^2T}}{\frac{1}{L^2}} = \frac{1}{L^2T}\frac{L^2}{1} = \frac{1}{T}$

$[\xi] = [\frac{a(7)}{a(1)}] = \frac{\frac{1}{LT^2}}{\frac{1}{L^2}} = \frac{1}{LT^2}\frac{L^2}{1} = \frac{L}{T^2}$ $\quad [\tau_2] = [\frac{b(1)}{b(2)}] = \frac{\frac{1}{L^2}}{\frac{1}{L^2T}} = \frac{1}{L^2}\frac{L^2T}{1} = T$

$[\delta_w] = [\frac{a(8)}{a(1)}] = \frac{\frac{1}{LT}}{\frac{1}{L^2}} = \frac{1}{LT}\frac{L^2}{1} = \frac{L}{T}$ $\quad [\delta_\Lambda] = [\frac{b(4)}{b(1)}] = \frac{\frac{1}{L}}{\frac{1}{L^2}} = \frac{1}{L}\frac{L^2}{1} = L$

Now we use the dimensions calculated above along with

$[X] = \frac{length^2}{time^2}$ $\quad [Y] = \frac{length^2}{time^2}$ $\quad [U] = \frac{length}{time}$ $\quad [\Psi_0] = length$ $\quad [\dot{\Psi}_0] = \frac{length}{time}$

in order to determine the dimensional homogeneity of the equations in the model:

$$\begin{aligned}
[\dot{X}] &= [\frac{-X}{\tau_1} - rY + sUY - \xi\Psi_0 + \delta_w\dot{\Psi}_0] \\
&= \frac{\frac{L^2}{T}}{T} - \frac{1}{T}\frac{L^2}{T} + \frac{1}{L}\frac{L}{T}\frac{L^2}{T} - \frac{L}{T^2}L + \frac{L}{T}\frac{L}{T} \\
&= \frac{L^2}{T^2} - \frac{L^2}{T^2} + \frac{L^2}{T^2} - \frac{L^2}{T^2} + \frac{L^2}{T^2}
\end{aligned}$$

$$
\begin{aligned}
[\dot{Y}] &= [\frac{-Y}{\tau_1} + rX - sUX + \zeta\Psi_0 U] \\
&= \frac{\frac{L^2}{T}}{T} + \frac{1}{T}\frac{L^2}{T} - \frac{1}{L}\frac{L}{T}\frac{L^2}{T} + \frac{1}{T}L\frac{L}{T} \\
&= \frac{L^2}{T^2} + \frac{L^2}{T^2} - \frac{L^2}{T^2} + \frac{L^2}{T^2}
\end{aligned}
$$

$$
\begin{aligned}
[\dot{U}] &= [\frac{-U}{\tau_2} + \frac{U_R}{\tau_2} - \eta\Psi_0 Y - \delta_\Lambda\dot{\Lambda}] \\
&= \frac{\frac{L}{T}}{T} + \frac{\frac{L}{T}}{T} - \frac{1}{TL^2}L\frac{L^2}{T} - L\frac{1}{T^2} \\
&= \frac{L}{T^2} + \frac{L}{T^2} - \frac{L}{T^2} - \frac{L}{T^2}
\end{aligned}
$$

As one can observe, $\dot{X}$, $\dot{Y}$, and $\dot{U}$ are dimensionally homogeneous. We confirmed Ruzmaikin's claim that $\dot{X}$ and $\dot{Y}$ both have dimension $\frac{L^2}{T^2}$ [7]. Now that we know the dimensions of the parameters and variables in the equations, this allows us to non-dimensionalize them. Non-dimensionalization gives us a huge advantage when solving the differential equations and building sensitivity functions because it reduces the computation time. In the next chapter we will develop and simulate all of the sensitivity functions.

CHAPTER 3

Sensitivity Analysis

In the paper by Ruzmaikin, *et al.*, the authors make the assumption that that the parameters h and Λ drive the dynamics of the system. Hence they assume that the other parameters are more robust, and do not significantly influence the dynamics of the system [7]. This assumption is justified by noting that most of the other parameters are well-fixed (*e.g.*, gravitational acceleration g). The overarching objective of my research is to test these claims, and see if Ruzmaikin's assumptions are justified. The following questions will drive my research:

- When does each parameter in the model exert significant influence on the overall dynamics?
- Which parameters in the model influence the long-term behavior most during the course of a simulation where each parameter value is chosen at random within the region of feasibility?

We will answer such questions by conducting a parameter sensitivity analysis, detailed in section 3.3.

Understanding which parameters drive the the most changes in the stratosphere will tremendously contribute to the work being done to understand what drives the changes in the northern hemisphere's polar vortex. Knowing which parameters we should try and understand more allows us to make studies of the atmosphere, in particular the stratosphere, more feasible by enabling the studies to be more focused, and direct, minimizing the tools necessary to conduct such research and thus, minimizing the costs associated with such research. Further, the sensitivity functions themselves can focus the data collection process by identifying when (during the course of a given season) we should try to collect data for the most relevant parameter values. This makes the parameter estimation process much more likely to be successful, since the data would be collected at a time when the system is most sensitive to changes in its value. If scientists are able to conduct studies and research that ultimately will provide us real life data, this data will serve to validate or debunk many of the existing atmospheric models. Another, more applicable advantage of my research is that by understanding this phenomena, (i.e., the polar vortex) individuals, organizations and agencies with existing efforts into reducing the anthropogenic contributions to climate change would be more informed and thus, their efforts would become more focused. Lastly, the outcomes of my research could help scientists in predicting what changes and behavior we should expect in the future, helping us better prepare for such life threatening events.

3.1 Sensitivity Functions

First, a numerical ODE solver in Matlab was used to solve the system of ordinary differential equations outlined in Chapter 2 with equations (1), (2), and (3). This will produce the appropriate functions for x, y, and u. Doing so will require that I simulate $\Lambda(t)$, $\dot{\Lambda}(t)$, Ψ_0, and $\dot{\Psi}_0$ appropriately, which was also performed in Matlab. We then build a dynamical system for the sensitivity functions associated with each parameter, enabling a thorough sensitivity analysis to be conducted in tandem with the original state variable equations.

Conducting a parameter sensitivity analysis allows us to, "evaluate the effects of parameter variations on the time course of model outputs and to identify the parameters to which the model is most/least sensitive." [2] Further, it will allow us to determine the optimal times for data collection, in that time periods of high sensitivity are more likely to provide useful information for estimating a particular parameter value.

In order to compute parameter sensitivity, we first compute the sensitivity functions associate with each parameter. The sensitivity functions for a generic parameter, say θ, and a differential equation of the form $\dot{x} = f(x;t;\theta)$ are defined as follows:

$$\dot{s}(t) = f_x s(t) + f_\theta \tag{4}$$

$$s(0) = 0, \tag{5}$$

where f would describe the right side of each differential equation (1), (2), and (3). Equation (5) denotes the suggested initial condition of 0 for the sensitivity functions. The derivatives of f with respect to x and θ are $f_x = \partial f/\partial x$ and $f_\theta = \partial f/\partial \theta$, respectively. Hence, I will have to calculate the partial derivatives of each differential equation with respect to each parameter, producing upwards of about 27 sensitivity functions. With these functions in hand, we are able to build a dynamical system for the sensitivity functions associated with each parameter [2].

First we need the partial derivative of (1), (2), and (3) with respect to x, y, and u, respectively. We get the following:

$$\frac{\partial \dot{X}}{\partial X} = -\frac{1}{\tau_1}, \frac{\partial \dot{Y}}{\partial Y} = -\frac{1}{\tau_1}, \frac{\partial \dot{U}}{\partial U} = -\frac{1}{\tau_2},$$

To illustrate our general process, we now display the development of the sensitivity functions for the parameter r.

$$\tfrac{\partial \dot{X}}{\partial r} = -Y \qquad \tfrac{\partial \dot{Y}}{\partial r} = X \qquad \tfrac{\partial \dot{U}}{\partial r} = 0$$

$$\Rightarrow \dot{S}_r^X = -\tfrac{1}{\tau_1} \times S_r^X - Y, \quad \dot{S}_r^Y = -\tfrac{1}{\tau_1} \times S_r^Y + X, \quad \dot{S}_r^U = -\tfrac{1}{\tau_2} \times S_r^U.$$

Since r only appears in the $\dot{X}$ and $\dot{Y}$ equations, it is expected that it does not have any impact on U. Hence the S_r^U plot is constantly zero, as observed in the next figure. Sensitivity for x and y increases in magnitude as time goes on.

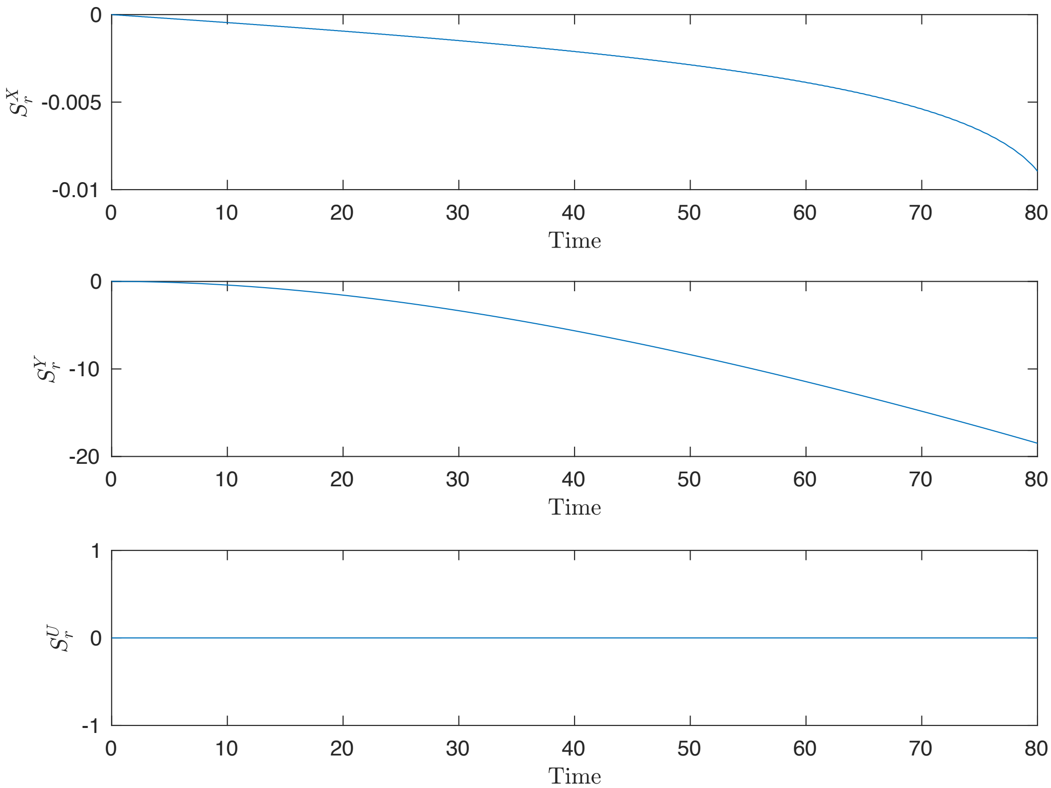

Figure 4: Sensitivities with respect to r

Next is the development of the sensitivity functions for the parameter s.

$$\frac{\partial \dot{X}}{\partial s} = UY \qquad \frac{\partial \dot{Y}}{\partial s} = -UX \qquad \frac{\partial \dot{U}}{\partial s} = 0$$

$$\dot{S}_s^X = -\frac{1}{\tau_1} \times S_s^X + UY \quad \dot{S}_s^Y = -\frac{1}{\tau_1} \times S_s^Y - UX \quad \dot{S}_s^U = -\frac{1}{\tau_2} \times S_s^U$$

Since s only appears in the $\dot{X}$ and $\dot{Y}$ equations, it is expected that there is no sensitivity with respect to it in U. Hence the S_s^U plot is constantly zero. It also holds very little influence on the other two state variables, only showing a moderate increase in magnitude as time goes on for the x-variable.

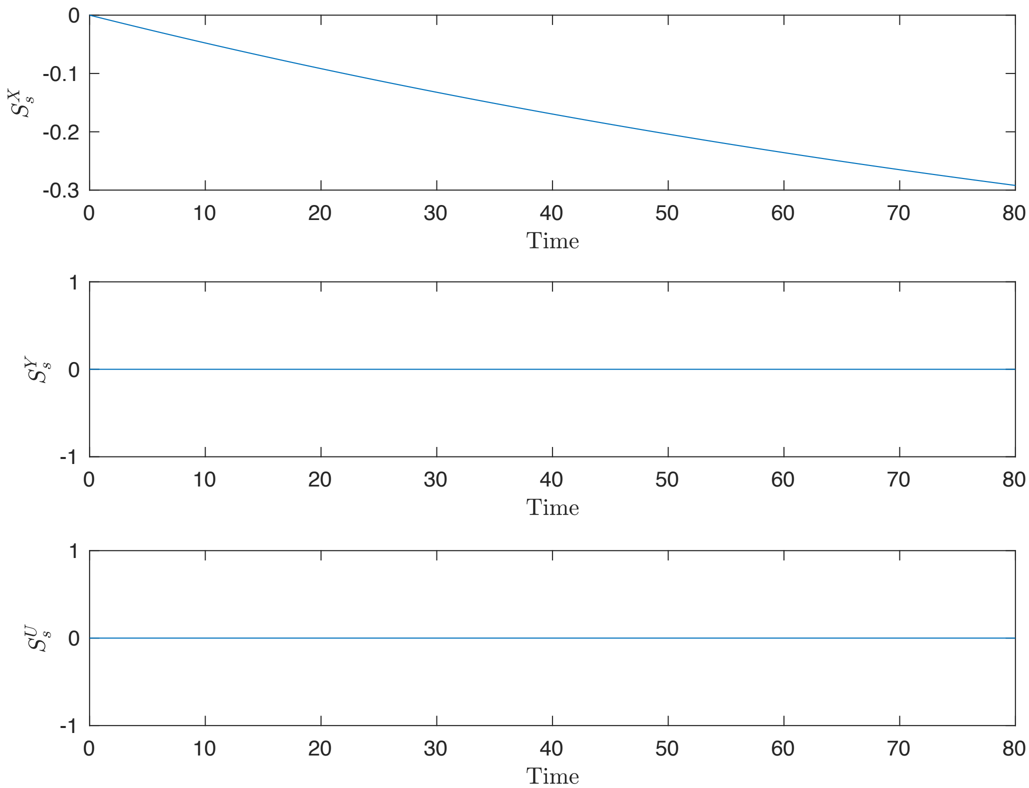

Figure 5: Sensitivities with respect to s

Now we examine the development of the sensitivity functions for the parameter τ_1, our first non-dimensionalized time parameter.

$$\frac{\partial \dot{X}}{\partial \tau_1} = -X \qquad \frac{\partial \dot{Y}}{\partial \tau_1} = -Y \qquad \frac{\partial \dot{U}}{\partial \tau_1} = 0$$

$$\dot{S}_{\tau_1}^X = -\frac{1}{\tau_1} \times S_{\tau_1}^X - X \quad \dot{S}_{\tau_1}^Y = -\frac{1}{\tau_1} \times S_{\tau_1}^Y - Y \quad \dot{S}_{\tau_1}^U = -\frac{1}{\tau_2} \times S_{\tau_1}^U$$

Since τ_1 only appears in the $\dot{X}$ and $\dot{Y}$ equations, it is expected that there is no sensitivity with respect to it in U. Hence the $S_{\tau_1}^U$ plot is constantly zero. Similar to the plots for the parameter r, we observe increasing sensitivity in the coordinate variables as time goes on.

In the development of the sensitivity functions for the parameter τ_2, we notice that many terms are identically zero, which has an obvious effect in our plots.

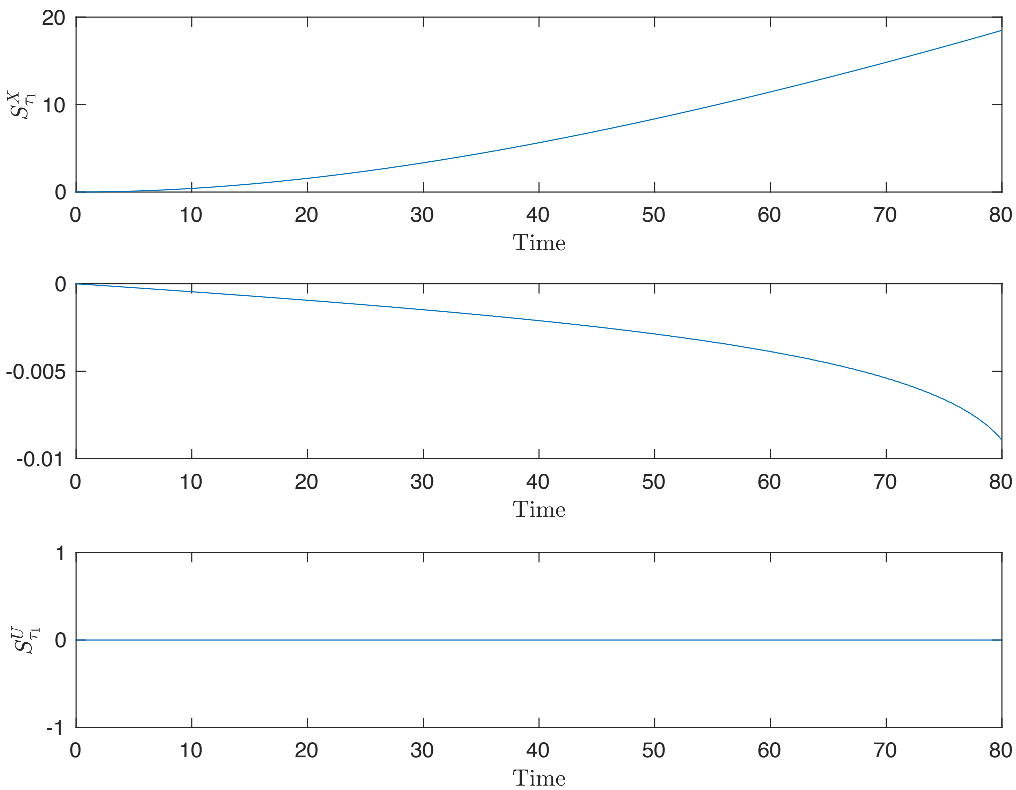

Figure 6: Sensitivities with respect to τ_1

$$\frac{\partial \dot{X}}{\partial \tau_2} = 0 \qquad \frac{\partial \dot{Y}}{\partial \tau_2} = 0 \qquad \frac{\partial \dot{U}}{\partial \tau_2} = -U + U_R$$

$$\dot{S}^X_{\tau_2} = -\frac{1}{\tau_1} \times S^X_{\tau_2} \quad \dot{S}^Y_{\tau_2} = -\frac{1}{\tau_1} \times S^Y_{\tau_2} \quad \dot{S}^U_{\tau_2} = -\frac{1}{\tau_2} \times S^U_{\tau_2} - U + U_R$$

Since τ_2 only appears in the $\dot{U}$ equation, it is expected that there is no sensitivity with respect to it in X or Y. Hence the $S^X_{\tau_2}$ and $S^Y_{\tau_2}$ plots are constantly zero in the next figure. We notice a moderate increase in sensitivity over time for the wind speed u.

For the parameter δ_w,

$$\frac{\partial \dot{X}}{\partial \delta_w} = \dot{\Psi}_0, \quad \frac{\partial \dot{Y}}{\partial \delta_w} = 0, \quad \text{and } \frac{\partial \dot{U}}{\partial \delta_w} = 0,$$

yielding the following sensitivity derivatives:

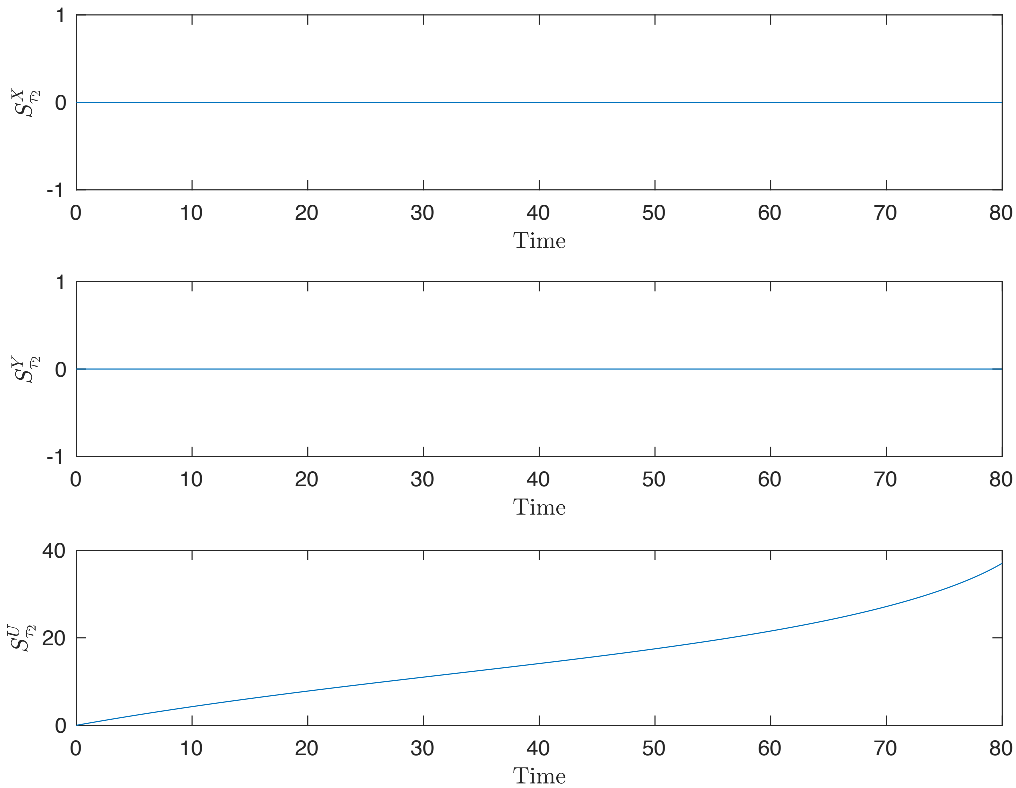

Figure 7: Sensitivities with respect to τ_2

$$\dot{S}^X_{\delta_w} = -\frac{1}{\tau_1} \times S^X_{\delta_w} + \dot{\Psi}_0, \quad \dot{S}^Y_{\delta_w} = -\frac{1}{\tau_1} \times S^Y_{\delta_w}, \quad \dot{S}^U_{\delta_w} = -\frac{1}{\tau_2} \times S^U_{\delta_w}.$$

Since δ_w only appears in the $\dot{X}$ equation, it is expected that there is no sensitivity with respect to it in Y or U. Hence the $S^Y_{\delta_w}$ and $S^U_{\delta_w}$ plots are constantly zero. Moreover, the sensitivity for the y-coordinate is so insignificant that all three plots appear to be constantly zero, so we omit them here.

Similarly we develop of the sensitivity functions for the parameter δ_Λ:

$$\frac{\partial \dot{X}}{\partial \delta_\Lambda} = 0 \qquad \frac{\partial \dot{Y}}{\partial \delta_\Lambda} = 0 \qquad \frac{\partial \dot{U}}{\partial \delta_\Lambda} = -\dot{\Lambda}$$

$$\dot{S}^X_{\delta_\Lambda} = -\frac{1}{\tau_1} \times S^X_{\delta_\Lambda} \quad \dot{S}^Y_{\delta_\Lambda} = -\frac{1}{\tau_1} \times S^Y_{\delta_\Lambda} \quad \dot{S}^U_{\delta_\Lambda} = -\frac{1}{\tau_2} \times S^U_{\delta_\Lambda} - \dot{\Lambda}$$

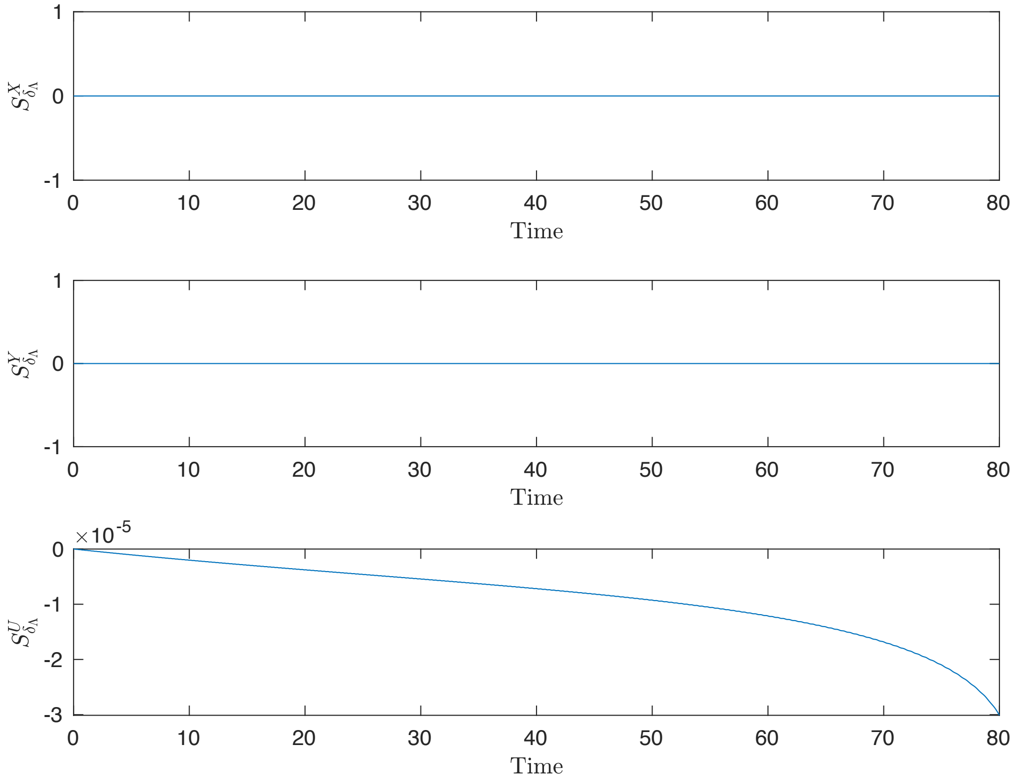

Figure 8: Sensitivities with respect to δ_Λ

Since δ_Λ only appears in the $\dot{U}$ equation, it is expected that there is no sensitivity with respect to it in X or Y. Hence the $S^X_{\delta_\Lambda}$ and $S^Y_{\delta_\Lambda}$ plots are constantly zero in the previous figure. As with δ_w, the third sensitivity plot also shows very little effect on the variable u, with only a very minor increase in magnitude as time goes on. It is worth noting that the sensitivity plots for the parameters δ_w and δ_Λ were somewhat surprising given their magnitude in comparison with other parameters in the model. This indicates that the choice of models for the functions Ψ_0 and Λ will have an extremely significant impact on the dynamics, so special attention is needed to correlate observable data with the functions used here.

Staying with the wind speed equation, we now present the development of the sensitivity functions for the parameter U_R.

$$\frac{\partial \dot{X}}{\partial U_R} = 0 \qquad \frac{\partial \dot{Y}}{\partial U_R} = 0 \qquad \frac{\partial \dot{U}}{\partial U_R} = \frac{1}{\tau_2}$$

$$\dot{S}^X_{U_R} = -\frac{1}{\tau_1} \times S^X_{U_R} \quad \dot{S}^Y_{U_R} = -\frac{1}{\tau_1} \times S^Y_{U_R} \quad \dot{S}^U_{U_R} = -\frac{1}{\tau_2} \times S^U_{U_R} + \frac{1}{\tau_2}$$

As with the previous parameter, U_R only appears in the wind speed equation and so there is no sensitivity with respect to the coordinate variables x and y. A small increase in sensitivity is observed over time with respect to the wind speed itself.

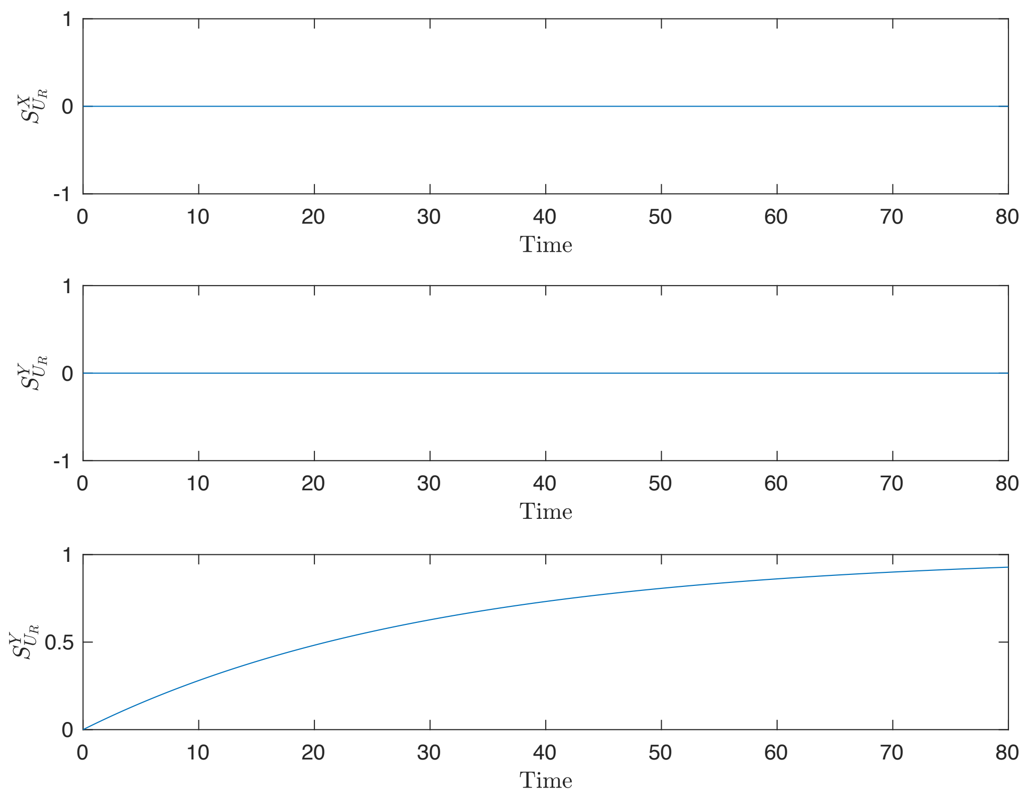

Figure 9: Sensitivities with respect to U_R

Continuing, we see a familiar patter in the development of the sensitivity functions for the parameter η:

$$\frac{\partial \dot{X}}{\partial \eta} = 0 \qquad\qquad \frac{\partial \dot{Y}}{\partial \eta} = 0 \qquad\qquad \frac{\partial \dot{U}}{\partial \eta} = -\Psi_0 Y$$

$$\dot{S}^X_\eta = -\frac{1}{\tau_1} \times S^X_\eta \quad \dot{S}^Y_\eta = -\frac{1}{\tau_1} \times S^Y_\eta \quad \dot{S}^U_\eta = -\frac{1}{\tau_2} \times S^U_\eta - \Psi_0 Y$$

Since η only appears in the $\dot{U}$ equation, it is expected that there is no sensitivity with respect to it in X or Y. Hence the S^X_η and S^Y_η plots are constantly zero in the figure. Again, there is also very little sensitivity with respect to the wind speed as well, further illustrating the strong impact in the choice of the model for $\Lambda(t)$.

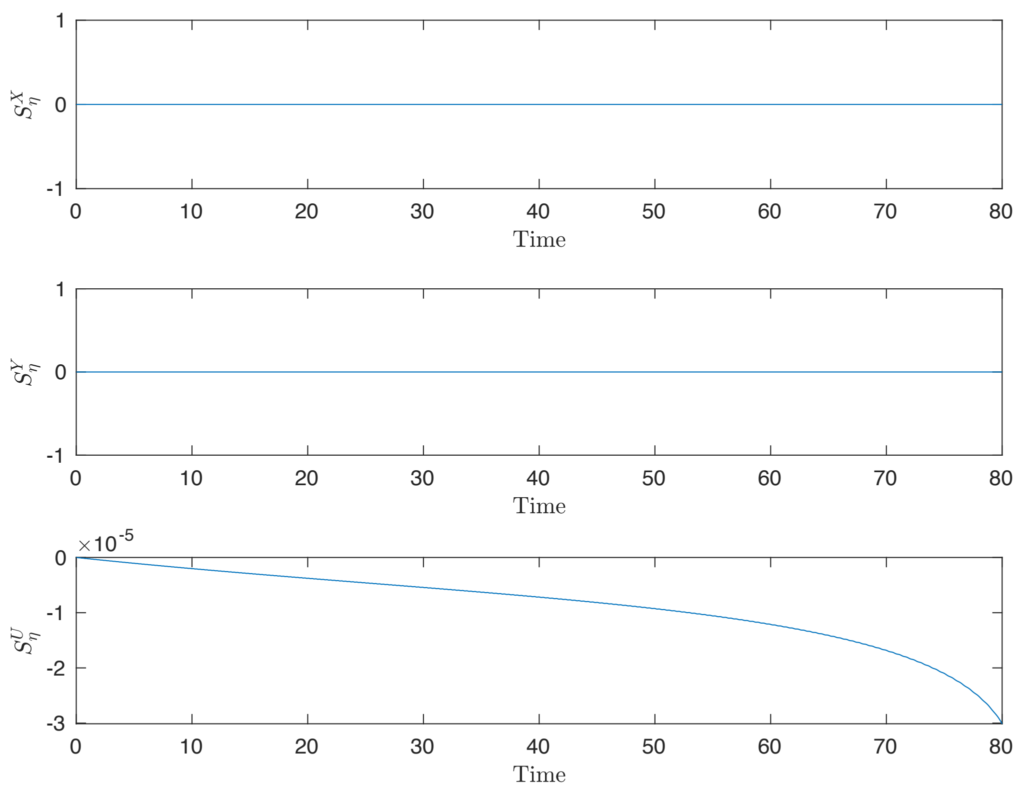

Figure 10: Sensitivities with respect to η

Moving back to the differential equation for the latitude coordinate, we have the development of the sensitivity functions for the parameter ζ:

$$\frac{\partial \dot{X}}{\partial \zeta} = 0 \qquad \frac{\partial \dot{Y}}{\partial \zeta} = \Psi_0 U \qquad \frac{\partial \dot{U}}{\partial \zeta} = 0$$

$$\dot{S}^X_\zeta = -\tfrac{1}{\tau_1} \times S^X_\zeta \quad \dot{S}^Y_\zeta = -\tfrac{1}{\tau_1} \times S^Y_\zeta + \Psi_0 U \quad \dot{S}^U_\zeta = -\tfrac{1}{\tau_2} \times S^U_\zeta$$

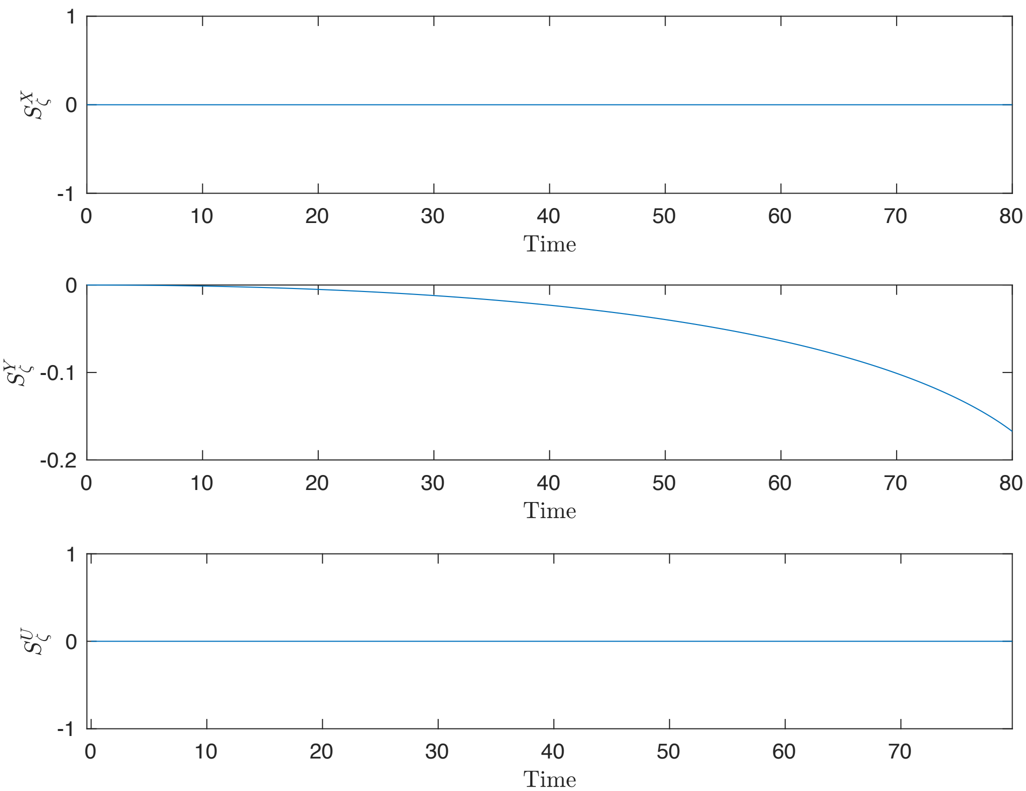

Figure 11: Sensitivities with respect to ζ

Since ζ only appears in the $\dot{Y}$ equation, it is expected that there is no sensitivity with respect to it in X or U. Hence the S^X_ζ and S^U_ζ plots are constantly zero in the figure. Only a small increase in the magnitude of the sensitivity occurs for S^Y_ζ as time goes on.

Finally, we present the development of the sensitivity functions for the parameter ξ:

$$\frac{\partial \dot{X}}{\partial \xi} = -\Psi_0 \qquad \frac{\partial \dot{Y}}{\partial \xi} = 0 \qquad \frac{\partial \dot{U}}{\partial \xi} = 0$$

$$\dot{S}^X_\xi = -\tfrac{1}{\tau_1} \times S^X_\xi - \Psi_0 \quad \dot{S}^Y_\xi = -\tfrac{1}{\tau_1} \times S^Y_\xi \quad \dot{S}^U_\xi = -\tfrac{1}{\tau_2} \times S^U_\xi$$

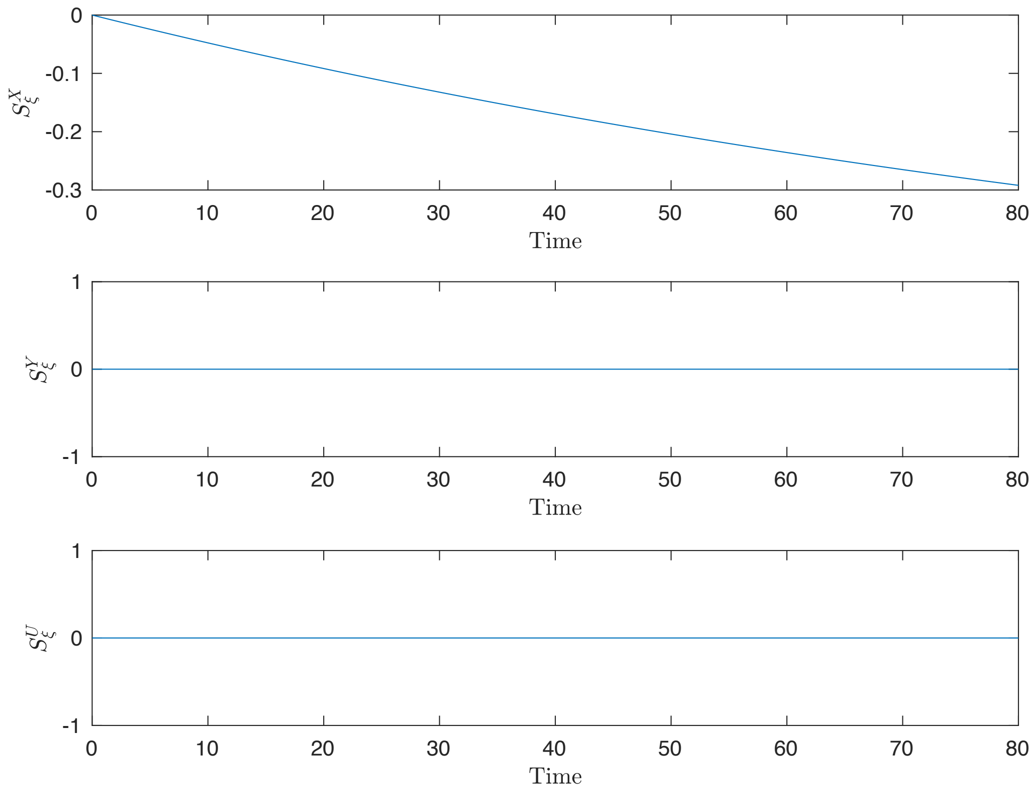

Figure 12: Sensitivities with respect to ξ

Since ξ only appears in the $\dot{X}$ equation, it is expected that there is no sensitivity with respect to it for Y or U. Hence the S_ξ^Y and S_ξ^U plots are constantly zero in the figure. A small increase in the magnitude of the sensitivity for the azimuthal coordinate is observed as times goes on.

Treating the function Ψ_0 as a constant given by its median value, we now develop the sensitivity functions for this as though it were a parameter in the model, similar to the approach taken in [7].

$$\frac{\partial \dot{X}}{\partial \Psi_0} = -\xi \qquad \frac{\partial \dot{Y}}{\partial \Psi_0} = \zeta U \qquad \frac{\partial \dot{U}}{\partial \Psi_0} = -\eta Y$$

$$\dot{S}^X_{\Psi_0} = -\frac{1}{\tau_1} \times S^X_{\Psi_0} - \xi \quad \dot{S}^Y_{\Psi_0} = -\frac{1}{\tau_1} \times S^Y_{\Psi_0} + \zeta U \quad \dot{S}^U_{\Psi_0} = -\frac{1}{\tau_2} \times S^U_{\Psi_0} - \eta Y$$

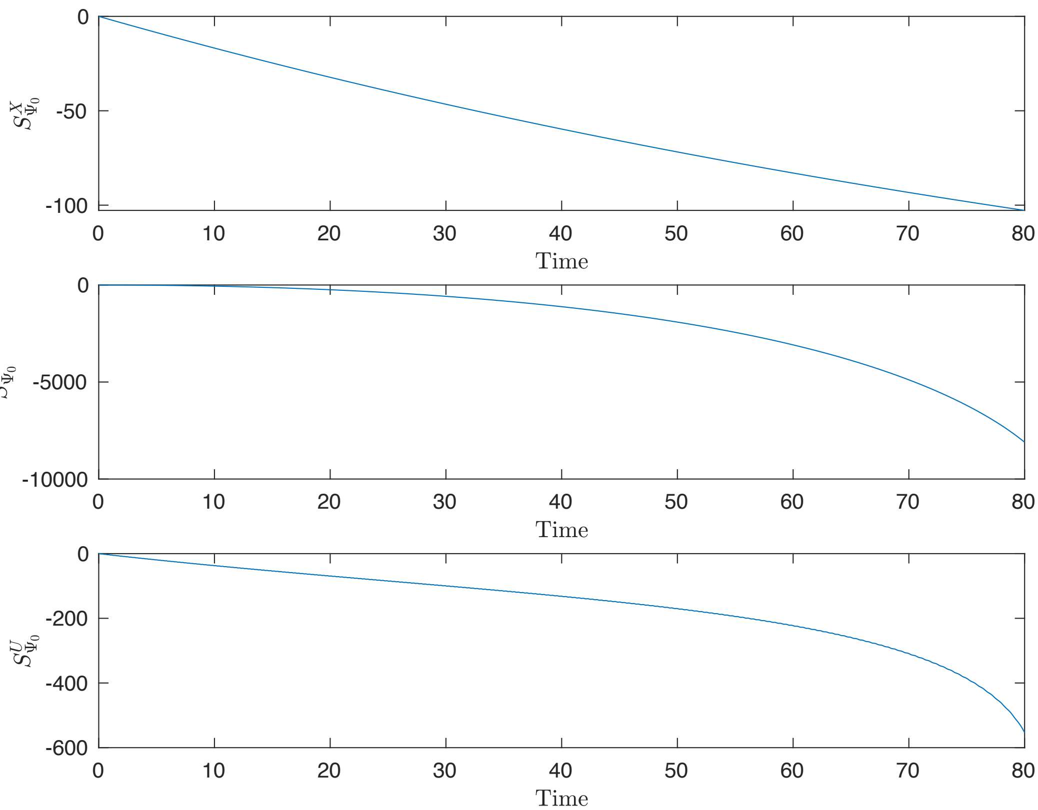

Figure 13: Sensitivities with respect to Ψ_0

Here we now see the significant impact of this function in all three differential equations, especially as time goes on.

Likewise, we can develop the sensitivity functions for $\dot{\Psi}_0$ by first computing the derivative of Ψ_0 and then substituting its median value.

$$\frac{\partial \dot{X}}{\partial \dot{\Psi}_0} = \delta_w \qquad \frac{\partial \dot{Y}}{\partial \dot{\Psi}_0} = 0 \qquad \frac{\partial \dot{U}}{\partial \dot{\Psi}_0} = 0$$

$$\dot{S}^X_{\dot{\Psi}_0} = -\frac{1}{\tau_1} \times S^X_{\dot{\Psi}_0} - \delta_w \quad \dot{S}^Y_{\dot{\Psi}_0} = -\frac{1}{\tau_1} \times S^Y_{\dot{\Psi}_0} \quad \dot{S}^U_{\dot{\Psi}_0} = -\frac{1}{\tau_2} \times S^U_{\dot{\Psi}_0}$$

Since $\dot{\Psi}_0$ only appears in $\dot{X}$, it is expected that there is no sensitivity with respect to it in Y or U. Hence the $S^Y_{\dot{\Psi}_0}$ and $S^U_{\dot{\Psi}_0}$ plots are constantly zero in the next figure. However, as with Ψ_0 itself, its time derivative will have a very strong impact on the dynamics of our azimuthal coordinate over time.

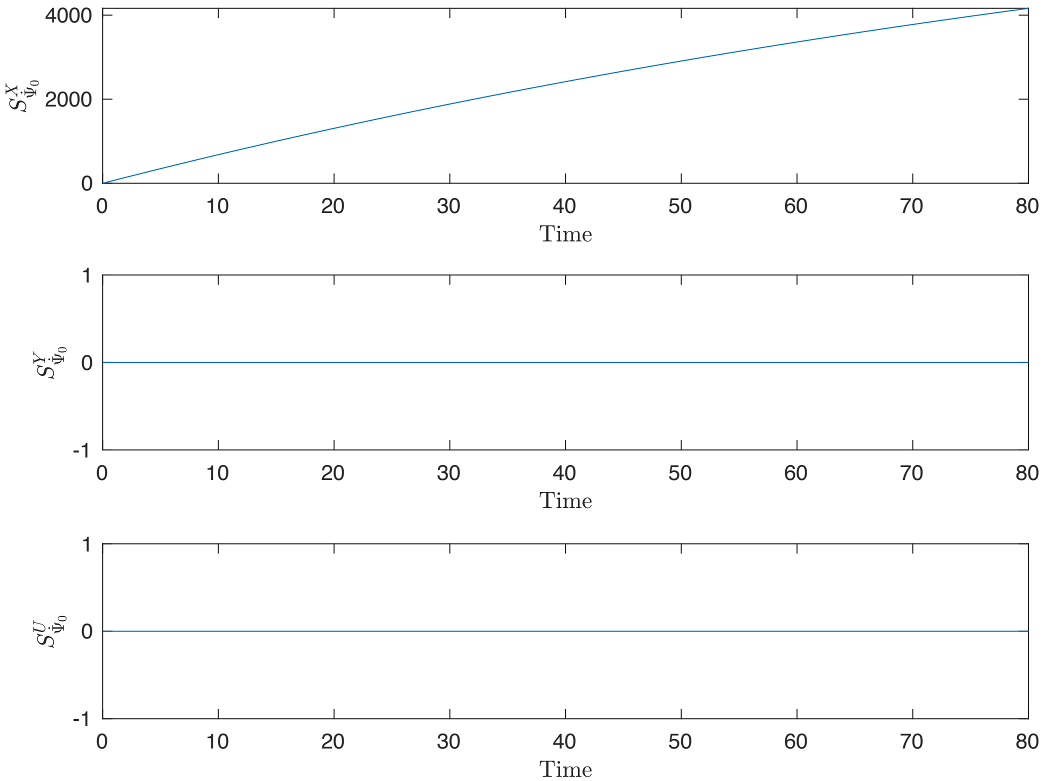

Figure 14: Sensitivities with respect to $\dot{\Psi}_0$

Finally, we develop the sensitivity functions for the function $\dot{\Lambda}$ by computing the derivative of $\Lambda(t)$ and taking its median value as a constant within our model:

$$\frac{\partial \dot{X}}{\partial \dot{\Lambda}} = 0 \qquad \frac{\partial \dot{Y}}{\partial \dot{\Lambda}} = 0 \qquad \frac{\partial \dot{U}}{\partial \dot{\Lambda}} = -\delta_\Lambda$$

$$\dot{S}^X_{\dot{\Lambda}} = -\frac{1}{\tau_1} \times S^X_{\dot{\Lambda}} \quad \dot{S}^Y_{\dot{\Lambda}} = -\frac{1}{\tau_1} \times S^Y_{\dot{\Lambda}} \quad \dot{S}^U_{\dot{\Lambda}} = -\frac{1}{\tau_2} \times S^U_{\dot{\Lambda}} - \delta_\Lambda$$

Since $\dot{\Lambda}$ only appears in $\dot{U}$, it is expected that there is no sensitivity with respect to it in X or Y. Hence the $S^X_{\dot{\Lambda}}$ and $S^Y_{\dot{\Lambda}}$ plots are constantly zero in the next figure. Only a minor increase in the magnitude of sensitivity is observed in the wind speed equation. This provides some justification for the choice in [7] to treat Λ as a constant and correlate it with the non-dimensional frequency r and the appropriate values for U_R in winter conditions. By doing

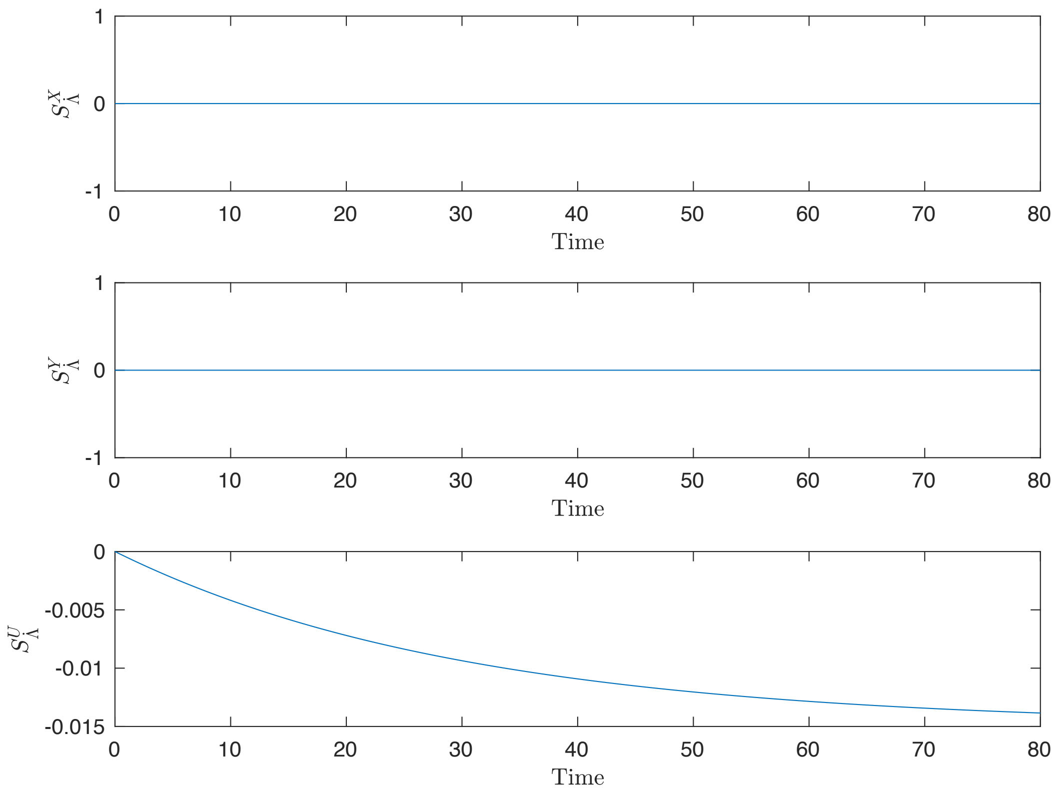

Figure 15: Sensitivities with respect to $\dot{\Lambda}$

this, their bifurcation analysis could then illustrate how key differences in the value of Λ led to different equilibrium solutions.

In the next chapter we will summarize our results from this sensitivity analysis and discuss the limitations we encountered during our study.

CHAPTER 4

Conclusions

In the paper by Ruzmaikin, *et al.*, they assumed that Λ and h have the most significant influence on the overall dynamics of the model. In the previous chapter, Figure 13 demonstrates how sensitive equations (1), (2), and (3) are with respect to Ψ_0. This observation validates the Ruzmaikin assumption regarding h, since $\Psi_0 = \frac{g}{f_0}h$. Due to the fact that Λ does not explicitly show up in any of the equations, we were unable to determine any direct sensitivity to it. Although, $\dot{\Lambda}$ is in $\dot{U}$ and so we were able to compute its sensitivity, which was of significantly lower magnitude.

We were also able to observe that Y grows in sensitivity with respect to r, whereas X is less sensitive. Overall, s strongly influences X. τ_1 mostly influences X, r mostly influences Y, and τ_2 has a significant influence on U.

Further, δ_Λ does not have significant influence on any of the equations. There is a very small influence on U. Similarly, δ_w has no influence on any of the equations. The parameters ξ, ζ, and similarly only have a very small influence on X, Y, and U, respectively.

Future work could include a sensitivity analysis on the initial conditions. Such work would allow us to know if there is always low sensitivity at first, as we have seen here, or if the initial conditions have a significant influence on the overall dynamics.

CHAPTER 5

Limitations

Throughout this study we faced a number of limitations, or shortcomings that we could not control. The first being a drastic difference in the time scale of the parameters. Physically, this makes sense. According to Saha, "motions in the atmosphere occur on different space and time scales." [8] Although mathematically this presents issues with calculations and accurate analysis, we were able to non-dimensionalize the parameters which helped to mitigate this time scale problem. Without doing so, the differential equations often tended to infinity and could not be solved. On this note, in [7], some of the parameter values were non-dimensionalized and some were not, without any specifications as to which were and which were not. This posed many problems when trying to solve the system because of the huge time scale differences. Performing the dimensional analysis and considering Justin Finkel's work in his paper *Path properties of climate transitions: a sudden stratospheric warming case study* simultaneously helped us solve this issue [3]. Once resolved, the Matlab code ran much faster and much more accurately.

Second, there were no given initial conditions for the differential equations in the system under study. Initial conditions specify a point that the solution curve (of the respective differential equation) passes through [6]. Hence, initial conditions are critical for solving the differential equation. To remedy this, we started each differential equation at zero.

As mentioned previously, $\Psi_0, \dot{\Psi}_0, \Lambda$ and $\dot{\Lambda}$ were not defined explicitly in Ruzmaikin's paper. Thus, we had to look back at other foundational papers to find such functions. Though we were successfully able to do so, which helped with conducting the dimensional analysis, we were unfortunately not able to include these functions in our sensitivity analysis. Our simulations there treat $\Psi_0, \dot{\Psi}_0, \Lambda$ and $\dot{\Lambda}$ as constant parameters. The values used were values listed in [7].

In Figure 2 and 3, at $t = 82.16502$ the equations reach an extremely large slope that caused our sensitivity solutions to tend to infinite magnitude. This resulted in Matlab producing an error. Hence we had to stop the sensitivity simulations at $t = 80$. Future work would include the use of an advanced stiff ODE solver that would provide better resolution.

REFERENCES

[1] D. G. Andrews, *An introduction to atmospheric physics*, Cambridge University Press, 2000.

[2] H. Banks, S. Dediu, and S. Ernstberger, *Sensitivity functions and their use in inverse problems*, Journal of Inverse and Ill-posed Problems **15** (2007).

[3] J. Finkel, *Path properties of climate transitions: a sudden stratospheric warming case study*, University of Chicago, 1–51.

[4] J. R. Holton and C. Mass, *Stratospheric vacillation cycles*, Journal of the Atmospheric Sciences **33** (1976), no. 11, 2218–2225.

[5] H. Kaper and H. Engler, *Mathematics and climate*, Society for Industrial and Applied Mathematics, 2013.

[6] J. D. Logan, *Applied mathematics*, 4th ed., Wiley, 2013.

[7] A. Ruzmaikin, J. Lawrence, and C. Cadavid, *A simple model of stratospheric dynamics including solar variability*, Journal of Climate **16** (2003), no. 10, 1593–1600.

[8] K. Saha, *The earth's atmosphere: Its physics and dynamics*, Springer-Verlag Berlin Heidelberg, 2008.

[9] D. W. Waugh, A. H. Sobel, and L. M. Polvani, *What is the polar vortex and how does it influence weather?*, Bulletin of the American Meteorological Society **98** (2017), no. 1, 37–44.

[10] S. Yoden, *Bifurcation properties of a stratospheric vacillation model*, Journal of the Atmospheric Sciences **44** (1987), no. 13, 1723–1733.

[11] ———, *An illustrative model of seasonal and interannual variations of the stratospheric circulation*, Journal of the Atmospheric Sciences **47** (1990), no. 15, 1845–1853.

VITA

Kiara Sanchez

EDUCATION

- Sam Houston State University, M.S. Mathematics, GPA 4.0, Expected May 2020
  Thesis: Parameter Sensitivity Analysis on a Model of Stratospheric Dynamics
- College of the Holy Cross, B.A. Mathematics & Minor in Educational Studies, GPA 3.22, May 2018

ACADEMIC EXPERIENCE

- Graduate Assistantship, Department of Mathematics and Statistics Sam Houston State University, Huntsville, TX, 2018-Present.
- Intern, Meetings and Professional Services, American Mathematical Society, Providence, RI, 2019.
- Private Tutor (AP Calculus AB), Self-Employed, Worcester, MA, 2018-2019.
- Student Teacher, Education Department, Doherty Memorial HS - College of the Holy Cross, Worcester, MA, 2017-2018.
- Notetaker, Office of Disability Services, College of the Holy Cross, Worcester, MA, 2017-2018.
- Teacher Assistant, ISLA Math Club, Latino Education Institute - Worcester State University, Worcester, MA, 2015-2016.

RESEARCH INTERESTS

- Applied Mathematics, Math and Climate, Dynamical Systems, Mathematics Education, Financial Math

CONFERENCES AND WORKSHOPS

- 2020 Joint Mathematics Meeting, American Mathematical Society, January 2020, Denver, CO

- The Field of Dreams Conference, The National Alliance for Doctoral Studies in Mathematics, November 2019, St. Louis, MO

- Mathematics & Climate Research Network Summer School and Academic Year Engagement Program, July 2019, American Institute of Mathematics and National Science Foundation, Durham, NC

- 2019 Industrial Mathematics/Statistics Modeling Workshop for Graduate Students, July 2019, The Statistical and Applied Mathematics Institute, North Carolina State University, Raleigh, NC

- 2019 Houston Summer School on Dynamical Systems, May 2019, The Department of Mathematics at the University of Houston, Houston, TX

- Critical Issues in Mathematics Education 2019: Mathematical Modeling in K-16: Community and Cultural Context, March 2019, Mathematical Sciences Research Institute, Berkeley, CA

- 10th biannual Blackwell-Tapia Conference, November 2018, Institute for Computational and Experimental Research in Mathematics, Providence, RI

- 2018 SACNAS - The National Diversity in STEM Conference, October 2018, Henry B. Gonzalez Convention Center, San Antonio, TX

GRANTS AND AWARDS

- American Mathematical Society
  2020 Travel Funds to work the BIG Career Center at the 2020 Joint Mathematics Meeting

- The Graduate School at Sam Houston State University
  2020 Travel Funds to attend the 2020 Joint Mathematics Meeting

- College of Science and Engineering Technology at Sam Houston State University
  2019 College of Science and Engineering Technology Graduate Achievement Scholarship

- The Graduate School at Sam Houston State University
  2019 The General Graduate School Scholarship

- The National Alliance for Doctoral Studies in Mathematics (Math Alliance)
  2019 Funding to attend the Field of Dreams Conference

- American Institute of Mathematics and the National Science Foundation
  2019 Funding for the MCRN Summer School and Academic Year Engagement Program

- The Statistical and Applied Mathematics Institute, North Carolina State University
  2019 Funding to attend the SAMSI 2019 IMSM Workshop for Graduate Students

- University of Houston
  2019 Funding to attend the 2019 Houston Summer School in Dynamical Systems

- Sam Houston State University
  2019 Graduate Student Appreciation Week Scholarship

- Sam Houston State University
  2019 Outstanding Graduate Student in Mathematics Award

- Mathematical Sciences Research Institute
  2019 Funding to attend the Critical Issues in Mathematics Education 2019 Workshop

- Institute for Computational and Experimental Research in Math, Brown University
  2018 Funding to attend 10th biannual Blackwell-Tapia Conference

- Dr. Luis Garcia, Sam Houston State University
  2018 Funding to attend 2018 SACNAS - The National Diversity in STEM Conference

- Sam Houston State University
  2018 Graduate Assistantship

- Sam Houston State University
  2018 Academic Success Program in Research Empowerment Scholarship

- College of the Holy Cross
  2014-2018 Pedro Arrupe, S.J. Scholarship

- IDEAL Industries
  2014-2018 Educational Scholarship

PRESENTATIONS

- Sanchez, K., Swim, E. (2019, April). Mathematical Modeling in College Algebra. Sam Houston State University. Huntsville, TX.

- Anifowoshe, F., Sanchez, K., Sterk Barrett, M. (2018, November). Being a racially minoritized female at Holy Cross: Young alumni perspectives. ENGAGE Summit. College of the Holy Cross. Worcester, MA.

PROFESSIONAL MEMBERSHIPS

- President, Sam Houston State University Chapter of American Mathematical Society